

Ricardo R. Ambriz
David Jaramillo
Gabriel Plascencia
Moussa Nait Abdelaziz *Editors*

Proceedings of the 17th International Conference on New Trends in Fatigue and Fracture

 Springer

**Proceedings of the 17th International Conference
on New Trends in Fatigue and Fracture**

Ricardo R. Ambriz · David Jaramillo
Gabriel Plascencia · Moussa Nait Abdelaziz
Editors

Proceedings of the 17th International Conference on New Trends in Fatigue and Fracture

Editors

Ricardo R. Ambriz
CIITEC-Instituto Politécnico Nacional
Mexico City
Mexico

Gabriel Plascencia
CIITEC-Instituto Politécnico Nacional
Mexico City
Mexico

David Jaramillo
CIITEC-Instituto Politécnico Nacional
Mexico City
Mexico

Moussa Nait Abdelaziz
Polytech' Lille
Université des Sciences et
Technologies de Lille
Villeneuve-d'Ascq
France

ISBN 978-3-319-70364-0 ISBN 978-3-319-70365-7 (eBook)
<https://doi.org/10.1007/978-3-319-70365-7>

Library of Congress Control Number: 2017959154

© Springer International Publishing AG 2018

This work is subject to copyright. All rights are reserved by the Publisher, whether the whole or part of the material is concerned, specifically the rights of translation, reprinting, reuse of illustrations, recitation, broadcasting, reproduction on microfilms or in any other physical way, and transmission or information storage and retrieval, electronic adaptation, computer software, or by similar or dissimilar methodology now known or hereafter developed.

The use of general descriptive names, registered names, trademarks, service marks, etc. in this publication does not imply, even in the absence of a specific statement, that such names are exempt from the relevant protective laws and regulations and therefore free for general use.

The publisher, the authors and the editors are safe to assume that the advice and information in this book are believed to be true and accurate at the date of publication. Neither the publisher nor the authors or the editors give a warranty, express or implied, with respect to the material contained herein or for any errors or omissions that may have been made. The publisher remains neutral with regard to jurisdictional claims in published maps and institutional affiliations.

Printed on acid-free paper

This Springer imprint is published by Springer Nature
The registered company is Springer International Publishing AG
The registered company address is: Gewerbestrasse 11, 6330 Cham, Switzerland

Contents

Theoretical and Experimental Analysis of the Energy Dissipation at Fatigue Crack Tip Under Cyclic Loading with Constant Stress Intensity Factor	1
O. Plekhov, A. Vshivkov and A. Iziumova	
A Study of Progressive Milling Technology on Surface Topography and Fatigue Properties of the High Strength Aluminum Alloy 7475-T7351	7
Miroslav Piska, Petra Ohnistova, Jana Hornikova and Charles Hervoches	
Study and Design of a New Range of Composite Based Shock Absorbers for the Automotive Sector	19
J. Niez, M. Ben Amara, J. Capelle, V. Bouchart and P. Chevrier	
A New High-Cycle Fatigue Criterion Based on a Self-consistent Scheme for Hard Metals Under Non-proportional Loading	29
Kékéli Amouzou and Eric Charkaluk	
Characterization and Evaluation of a Railway Wheel Steel in the HCF and VHCF Regimes	41
Henrique Soares, Pedro Costa, Mário Vieira, Manuel Freitas and Luís Reis	
High-Temperature Low Cycle Fatigue Resistance of Inconel 713LC Coated with Novel Thermal Barrier Coating	49
Ivo Šulák, Karel Obrtlík, Ladislav Čelko, David Jech and Pavel Gejdoš	
The Effect of Pearlite Banding on the Mechanical Anisotropy of Low Carbon Steel	57
M. Beltrán, J. L. González, D. I. Rivas, Felipe Hernández and Héctor Dorantes	

Analysis of Mechanical Behavior of the Underlying Soft Tissue to Ischial Tuberosities Using Finite Element Method	67
Diana Alicia Gayol-Mérida, Víctor Manuel Araujo-Monsalvo, José de Jesús Silva-Lomelí, Víctor Manuel Domínguez-Hernández, Marcos Martínez-Cruz, Elisa Martínez-Coría, Martín Luna-Méndez and Ayleneid Alemán-Pérez	
Study of the Endurance Limit of AA7075 Aluminum Produced by High-Pressure Vacuum Die Casting Analyzed by Classical Whöler Curve	75
David Levasseur, Jimmy Simard, Francis Breton and Lotfi Toubal	
Life Prediction of a Mono Contact Aluminum/Steel at Constant and Variable Amplitudes Loading in Fretting Fatigue Configuration	85
A. Belloula, A. Amrouche and M. Nait-Abdelaziz	
Influence of Microstructure on Fatigue Crack Formation and Growth in a Low-Carbon Steel	91
Donka Angelova, Rozina Yordanova and Svetla Yankova	
Determination of the Region of Stabilization of Low-Cycle Fatigue HSLE Steel from Test Data	101
Bojana Aleksić, Vujadin Aleksić, Abubakr Hemer, Ljubica Milović and Aleksandar Grbović	
Study of a Stud Bolt Wrench Failure Due to an Inadequate Heat Treatment.	113
Sandra L. Rodriguez-Reyna, Francisco G. Perez-Gutierrez, J. Luis Hernández-Rivera, Jorge Zaragoza-Siqueiros and Christian J. Garcia-Lopez	
Multiaxial Fatigue of Rubbers: Comparative Study Between Predictive Tools	123
G. Ayoub, M. Naït Abdelaziz and F. Zaïri	
Laboratory Study of Fatigue in Water Conveying HDPE and PVC Pipes Subject to Extreme Hydraulic Transient Pressures	129
René Autrique Ruiz and Eduardo Antonio Rodal Canales	
Probabilistic Assessment of Nuclear Piping Integrity by Considering Environmental Fatigue and Stress Corrosion Cracking	139
Seung Hyun Kim, Md Nasimul Goni and Yoon-Suk Chang	
The Inspections, Standards and Repairing Methods for Pipeline with Composite: A Review and Case Study	147
M. Hadj Meliani, O. Bouledroua, Z. Azari, A. Sorour, N. Merah and G. Pluinage	

Effect of Microstructure on Tension, Charpy and DWTT Properties on Two API X70 Plates	157
Fernando Guzmán, Moisés Hinojosa and Eduardo Frias	
Fatigue Analysis in a Bellow Expansion Joint Installed a Heat Exchanger	165
I. Villagómez, J. L. González, J. J. Trujillo and D. Rivas	
Failure Analysis of Stress Corrosion Cracking of a Ball Valve in Service	173
I. Mortera, J. L. González, A. Casarrubias and D. Rivas	
Assessment of Danger Due to Cracks in Structural Elements of Different Shapes and Geometry	181
Orest Bilyy	
Formation of Preferential Paths in Cracked Hele-Shaw Cells by Water Injection—An Experimental Study	189
S. de Santiago, I. V. Lijanova, C. O. Olivares-Xometl and N. V. Likhanova	
Smith Watson and Topper Model in the Determination of the Fatigue Life of an Automotive Steel	197
F. F. Curiel, R. R. Ambriz, M. A. García, M. C. Ramírez and S. García	
Influence of Weld Parameters and Filler-Wire on Fatigue Behavior of MIG-Welded Al-5083 Alloy	209
Vidit Gaur, Manabu Enoki, Toshiya Okada and Syohei Yomogida	
Mechanical Evaluation of IN718-AL6XN Dissimilar Weldment	215
R. Cortés, R. R. Ambriz, V. H. López, E. R. Barragán, A. Ruiz and D. Jaramillo	
Fatigue Life of Resistance Spot Welding on Dual-Phase Steels	225
J. H. Ordoñez Lara, R. R. Ambriz, C. García, G. Plascencia and D. Jaramillo	
Failure Analysis by Hot Cracking Root HAZ in Welding SMAW Type	237
M. Arzola, J. L. González, S. J. García, D. I. Rivas and E. Sandoval	
Effect of Electromagnetic Field on the Microstructure and Mechanical Properties of the Dissimilar 2205/316L Welded Joint	247
S. L. Hernández-Trujillo, V. H. López-Morelos, R. García-Hernández, M. A. García-Rentería, A. Ruiz-Marines and J. A. Verduzco-Martínez	
Heat Input Effect on the Mechanical Properties of Inconel 718 Gas Tungsten Arc Welds	255
N. K. Rodríguez, E. R. Barragán, I. V. Lijanova, R. Cortés, R. R. Ambriz, C. Méndez and D. Jaramillo	

A Case Study of Corrosion Fatigue in Aluminium	
Casing Bolt Holes	263
Siew Fong Choy	
Study of the Modal Effect of 1045 Steel Pre-stressed Beams Subjected to Residual Stress	269
Erasto Vergara Hernández, Brenda Carolina Pérez Millán, Juan Manuel Sandoval Pineda and Luis Armando Flores Herrera	
Experimental Analysis of Fatigue Cracks Emanating from Corner Notches in the Presence of Variable Residual Stress Fields	273
J. L. Cuevas, C. Garcia, A. Amrouche, R. R. Ambriz and D. Jaramillo	
Fatigue Crack Initiation and Growth on Welded Joints of 2205 Duplex Alloy: The Effect of Electromagnetic Interaction During Welding	281
J. Rosado-Carrasco, J. González-Sánchez, V. H. López-Morelos and G. R. Domínguez	
Nondestructive Monitoring of Rail Surface Damage Via Barkhausen Noise Technique	287
M. Neslušán, K. Zgútová, I. Maňková, P. Kejzlar and J. Čapek	
Failure Analysis of Stress Corrosion Cracking of Two Tees in a Pressurized Drainage System	299
D. Rivas, J. L. González, A. Casarrubias and M. Beltran	
Fatigue Life Extension of 2205 Duplex Stainless Steel by Laser Shock Processing: Simulation and Experimentation	307
V. Granados-Alejo, C. A. Vázquez-Jiménez, C. Rubio-González and G. Gómez-Rosas	
Fracture Toughness of Fiber Metal Laminates Through the Concepts of Stiffness and Strain-Intensity-Factor	313
Jesús Gerardo Martínez Figueroa and Perla Itzel Alcántara Llanas	
Uncertainty Quantification of Fatigue Life Prediction in Welded Structures Using Microstructure-Based Simulations	329
Takayuki Shiraiwa, Fabien Briffod and Manabu Enoki	
Prediction of Fatigue Life Induced by Defects Considering Crack Initiation	335
Ryota Sakaguchi, Takayuki Shiraiwa and Manabu Enoki	
Peridynamic Modeling of Cracking in Ceramic Matrix Composites	341
Yile Hu, Erdogan Madenci and Nam Phan	
Evaluation of Stress Intensity Factors (SIFs) Using Extended Finite Element Method (XFEM)	355
Bojana Aleksić, Aleksandar Grbović, Abubakr Hemer, Ljubica Milović and Vujadin Aleksić	

Determination of the Region of Stabilization of Low-Cycle Fatigue HSLE Steel from Test Data

Bojana Aleksić, Vujadin Aleksić, Abubakr Hemer,
Ljubica Milović and Aleksandar Grbović

Introduction

The most important role in fracture of the materials of machine parts and structures has various types of fatigue. The fatigue life of reliable components of engineering elements, such as bearings, which are exposed to variable load over the life of exploitation, can be estimated by the analysis of the behaviour that includes processing of the data on loading, geometry and the material selected for manufacture of the bearings, both by simulation and experimentally [1–5].

Steel, NN-70, selected in this study to investigate the experimental behaviour affected by fatigue loading, among other things, is used in shipbuilding and for manufacture of pressure vessels as well. The experiment was conducted using smooth round specimens made of steel NN-70 as parent material (PM). When selecting stabilized hysteresis as a representative of all of stabilized hysteresis for one strain level, and for the further processing of low-cycle fatigue test results, the recommendations of standards [6, 7] have been used as well as the methodology

B. Aleksić (✉)

Innovation Centre of Faculty of Technology and Metallurgy,
Karnigijeva 4, 11120 Belgrade, Serbia
e-mail: baleksic@tmf.bg.ac.rs

V. Aleksić

Institute for Testing Materials—IMS Institute, Bulevar vojvode Mišića 43,
11000 Belgrade, Serbia

A. Hemer · L. Milović

Faculty of Technology and Metallurgy, University of Belgrade,
Karnigijeva 4, 11120 Belgrade, Serbia

A. Grbović

Faculty of Mechanical Engineering, University of Belgrade,
Kraljice Marije 16, 11120 Belgrade, Serbia

© Springer International Publishing AG 2018

R. R. Ambriz et al. (eds.), *Proceedings of the 17th International Conference on New Trends in Fatigue and Fracture*, https://doi.org/10.1007/978-3-319-70365-7_12

based on which linearity of the stabilization regions of low-cycle fatigue was numerically determined [8].

Background and Characteristics of Steel NN-70

Parent material (PM) used to make the test specimens was a plate of the dimensions (45 × 205 × 353) mm made of low-alloy high-strength steel NN-70 with properties shown in Tables 1 and 2.

Steel NN-70 is the Yugoslav version of American steel HY-100 and is intended for manufacture of ship structures, submarines and pressure vessels by welding, where the required toughness is extremely important. The technology of manufacture and thermomechanical processing (TMCP steels [10]) of the steel called Nionikral-70 is the result of joint research work of the metallurgists of Military Technical Institute in Žarkovo (VTI) and the steelworks “Jesenice” from Jesenice [11], in the early 90s of the last century. It was made in the electric furnace, cast in brams, subsequently rolled into slabs and finally the sheets of various thicknesses. Due to some of its characteristics, it is classified among the fine-grained steels. The process of hardening is the combination of classical improvement (quenching and tempering) with grain refinement in accordance with selected chemical composition, by micro-alloying and appropriate deposition [12]. In determining the limit values of carbon and other alloying elements for the analysis, bearing in mind the purpose of the steel, care was taken to meet the requirements for the combination of characteristics such as strength, ductility, resistance to crack initiation and propagation, the stability of these properties at low temperatures, good resistance to fatigue and stress corrosion, and good workability and weldability [12]. Steel NN-70 is intended to be shaped by welding, so that after it was successfully mastered, its suitability for welding was also subjected to assessment [11].

Table 1 Chemical composition of NIONIKRAL 70, %wt [8]

C	Si	Mn	P	S	Cr
0.106	0.209	0.220	0.005	0.0172	1.2575
Ni	Mo	V	Al	As	Sn
2.361	0.305	0.052	0.007	0.017	0.014
Cu	Ti	Nb	Ca	B	Pb
0.246	0.002	0.007	0.0003	0	0.0009
W	Sb	Ta	Co	N	–
0.0109	0.007	0.0009	0.0189	0.0096	–

Table 2 Mechanical properties of NIONIKRAL 70 [8]

Property	PM
Ultimate tensile strength, MPa	855, rounded value
Yield strength, MPa	815, rounded value
Elastic modulus, GPa	221.4, dynamic, LCF
Impact toughness, J	97, rounded value, 20 °C
E initiation, J	40, rounded value, 20 °C
E propagation, J	57, rounded value, 20 °C
HV30, plate of PM	257, mean value, plate of PM
HV10, stick for LCF specimen [9]	257, mean value, specimen of LCF

Testing of Steel NN-70 at Low-Cycle Fatigue

From the necessity to assess the low-cycle fatigue life, and in order to determine the fatigue characteristics of the material, the test of resistance of the parent material (PM) of steel NN-70 to low-cycle fatigue was carried out. Preparation of the test of resistance of steel NN-70 to low-cycle fatigue consisted of making smooth cylindrical specimens, Fig. 1 item 1, and tool for placing the specimens in the tearing-machine jaw, Fig. 1 items 2 and 3, and check of the target static tensile properties of steel NN-70, Table 2.

The procedure for determination of the low-cycle fatigue characteristics and geometry of cylindrical smooth specimen as well, Fig. 1 item 1, is defined by the ISO 12106:2003(E) [6] and ASTM E 606-04^e [7] standards.

Fatigue test was conducted on a universal MTS system (Material Testing System—Universal hydraulic dynamic tearing machine of 500 kN) for the material testing, schematically presented by photos in Fig. 2.

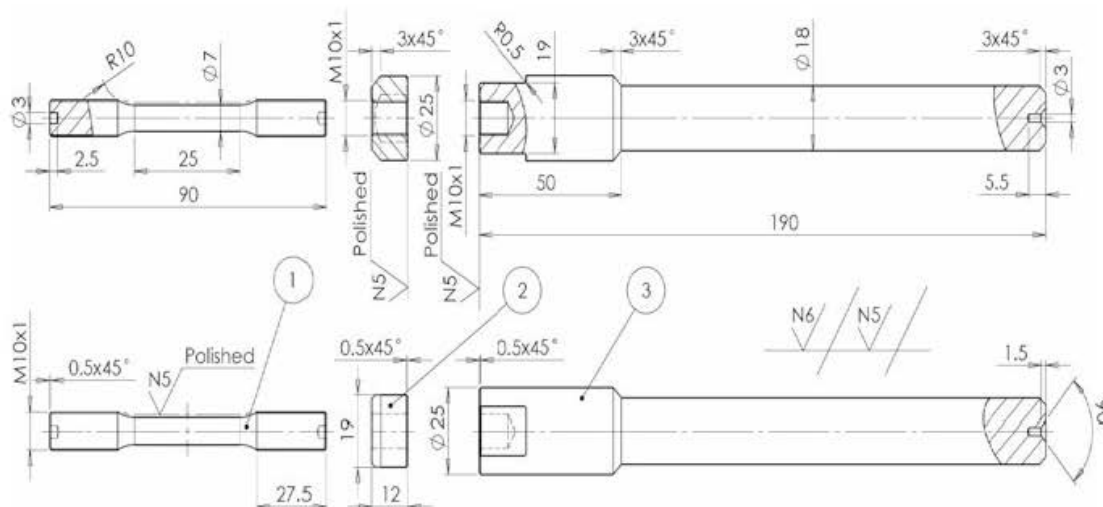


Fig. 1 Specimen and specimen holder for testing LCF of steel NN-70 [8]. Item 1, LCF specimen, NN-70, D = 7 mm; item 2, Jam nut, 42CrMo4; item 3, Grip holder, 42CrMo4.

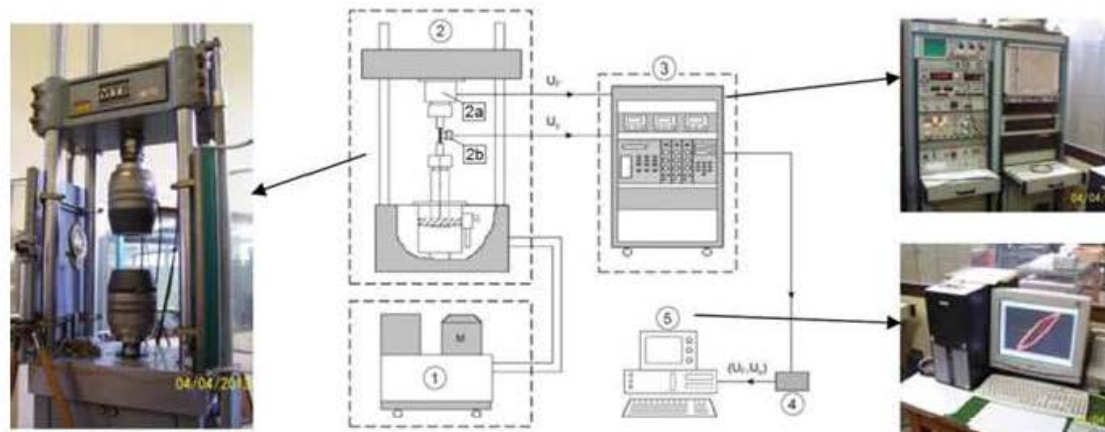


Fig. 2 MTS universal system for the material testing, 1—Hydraulic aggregate, 2—Pulsating device, 2a—MTS force-feeding device, 2b—MTS extensometer, 3—Control system, 4—A/D convertor, 5—PC

Used MTS force-feeding device, Fig. 2 item 2a, with linear characteristics $F[\text{kN}] = F[\text{V}] \cdot 10$, and MTS extensometer with measuring length of $L_0 = 25$ mm, Fig. 2 item 2b with linear characteristics $\varepsilon[\%] = \varepsilon[\text{V}] \cdot 0.2$, are graphically presented in Fig. 2.

Low-cycle fatigue tests were performed on a series of smooth specimens made of steel NN-70, with semi-amplitudes of controlled and fully reversible strains, $\Delta\varepsilon/2 = 0.35, 0.45, 0.50, 0.60, 0.70$ and 0.80 ($\Delta\varepsilon/2 = \text{const}$, $R_\varepsilon = \varepsilon_{\min}/\varepsilon_{\max} = -1$).

Numerical Determination of the Region of Stabilization

Most of the materials, at low-cycle fatigue and at a certain level regulated strain, achieve a so-called stabilized condition. It is a condition when the height of the hysteresis loop expressed through a range of force of loading or stress slightly changes, Fig. 3 item 9.

The most common methods for determination of the number of cycles to crack initiation, N_f , are defined by the standards [6, 7]. New methods [8] for determination of the beginning and end of the crack initiation and establishment of linearity of stabilization regions are based on experimental data, by arbitrary selection of three cycles on the basis of which we can establish linearity that we maintain by filtering the data in the programme EXCEL, toward the beginning and end of the test. The results of established linearity in the areas of stabilization for steel NN-70 are shown in Table 3.

In this way we determine the initial, N_{bs} , and final, N_{es} , cycle of stabilization, i.e. the beginning and end of the crack initiation, Fig. 4a. Stabilized hysteresis, N_{s1} , Fig. 4b, is located in the middle of the region 9, Fig. 3, and is determined by the formula, $N_{s1} = N_{bs} + (N_{es} - N_{bs})/2$. This method of determination of the stabilized hysteresis, N_{s1} , is called “Method of the middle stabilization (ms)” [8]. In a similar

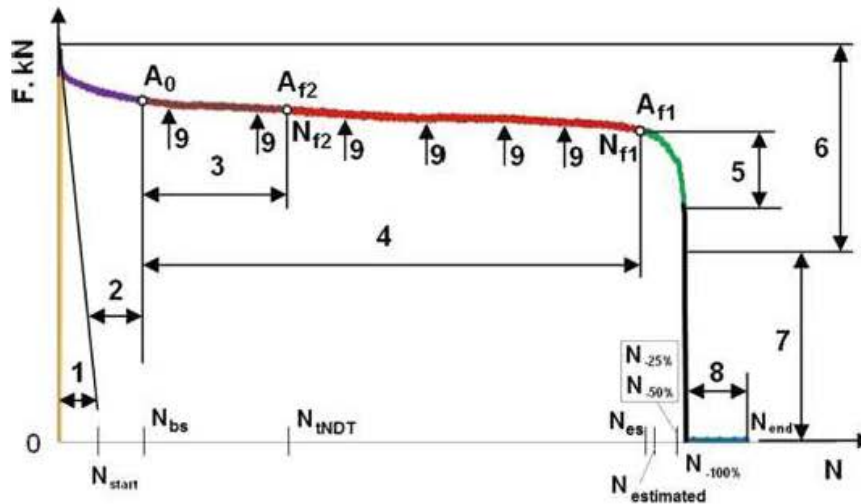


Fig. 3 Regions of low-cycle fatigue. 1—Adjustment of tearing machine, 2—Adaptation of tearing machine, tools and specimen, 3—Crack formation up to threshold of NDT, 4—Stabilized state, 5—Force drop of 25 % (ISO 12106:2003(E)) [6], 6—Force drop of 50 % (ASTM E 606-04) [7], 7—Force drop to $F = 0$, 8—Stoppage of tearing machine, 9—Height of hysteresis loop, N_{start} —Test start up, F_{max} , N_{bs} —Beginning of stabilization, A_0 , mm, N_{INDT} —threshold of the NDT, A_{f2} , mm, N_{es} —End of stabilization, A_{f1} , mm, $N_{estimated}$ —force-drop assessment of an operator, N_{end} —Test termination, A_0 —initial cross-section of the specimen (css), A_{f1} —css at the end of stabilization, A_{f2} —css at the threshold of the NDT

way, we can establish a cycle of appearance of a crack of 1 mm^2 surface area [13], which can be identified by the NDT methods, which is called the “threshold NDT method (tNDT)” [8], and then the cycle of stabilized hysteresis, N_{s2} , Fig. 4b, which is located in the middle of the region 3, Fig. 3, so that $N_{s2} = N_{bs} + (N_{INDT} - N_{bs})/2$. This procedure was applied to other specimens as well, i.e. other strain levels, $\Delta\varepsilon/2 = 0.35, 0.45, 0.50, 0.60, 0.70$ and 0.80 .

The accuracy of determination of the exponents and coefficients of cyclic stress-strain curve (CSSC) and basic curve of low-cycle fatigue (BCLCF) depends on accuracy of determination of linearity of stabilization region (for 7 samples, determination coefficient, $R^2 = 0.85\text{--}0.98$, Table 3) and for chosen method for determination of the stabilization curve it ranges as follows: for CSSC (for ms method for determination of n' and K' it is $R^2 = 0.66$, and for tNDT method it is $R^2 = 0.62$, Table 4, while for BCLCF (for ms method for determination b and σ_f' it is $R^2 = 0.77$, and tNDT it is $R^2 = 0.78$, Table 4) (for ms method for determination of c and ε_f' $R^2 = 0.72$ and for tNDT method $R^2 = 0.68$, Table 4).

After processing of registered data from all stabilized hysteresis of interest obtained using the methodology described, the curves of low-cycle fatigue for steel NN-70 are defined [14]:

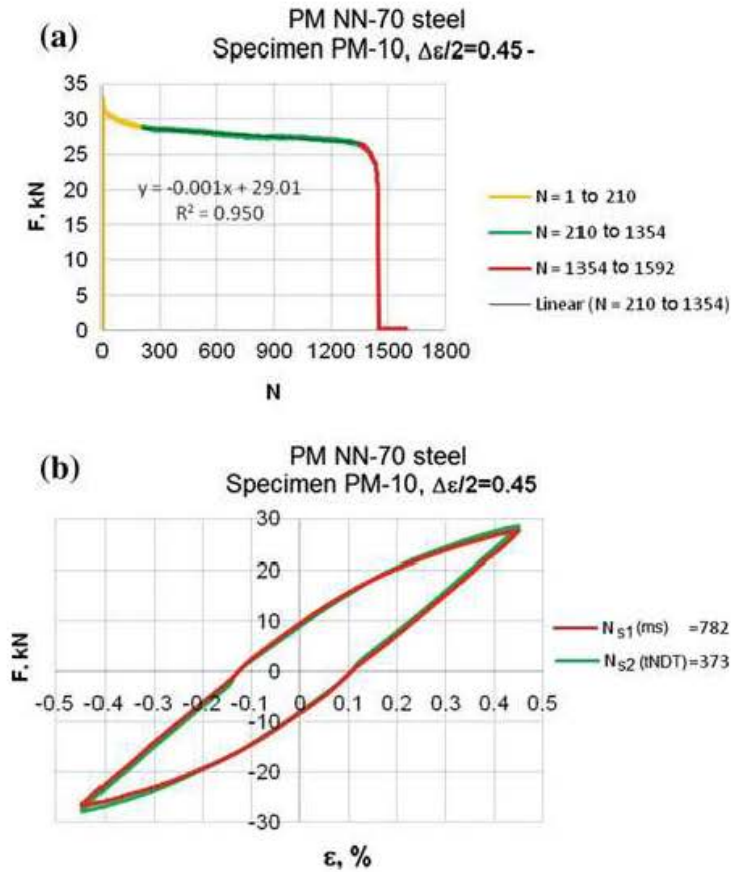
Table 3 Data on the area of stabilization and characteristic cycles of LCF for PM of steel NN-70

Specimen	$\Delta\varepsilon/2\%$	Stabilization regions		Characteristic cycle of stabilization					
		$y = F, \text{ kN}; x = N$	R^2	N_{bs}	$N_{t_{NDT}} = N_{f2}$	${}^bN_{s2}$	$N_{es} = N_{f1}$	${}^aN_{s1}$	
PM-01	0.35	$y = -0.002x + 26.77$	0.98	385	668	527	948	667	
PM-10	0.45	$y = -0.001x + 29.01$	0.95	210	535	373	1354	782	Figure 4
PM-03	0.50	$y = -0.002x + 28.57$	0.97	256	575	416	1271	764	
PM-06	0.60	$y = -0.005x + 29.65$	0.94	127	261	194	415	271	
PM-07	0.60	$y = -0.006x + 29.84$	0.90	97	210	154	293	195	
PM-05	0.70	$y = -0.006x + 29.04$	0.91	135	272	204	333	234	
PM-08	0.80	$y = -0.013x + 30.47$	0.85	82	142	112	165	124	

$${}^aN_{s1} = N_{bs} + (N_{es} - N_{bs})/2$$

$${}^bN_{s2} = N_{bs} + (N_{t_{NDT}} - N_{bs})/2$$

Fig. 4 a The region of stabilization, $N = 210$ to 1354 and b stabilized hysteresis in cycles $N_{s1} = N_s(ms) = 782$ and $N_{s2} = N_s(tNDT) = 373$



Cyclic stress-strain curves,

$$\frac{\Delta \epsilon}{2} = \frac{\Delta \sigma}{2E} + \left(\frac{\Delta \sigma}{2K'} \right)^{\frac{1}{n'}} :$$

$$\text{for } \underline{N_{s1}} : \frac{\Delta \epsilon}{2} = \frac{1}{221378} \cdot \frac{\Delta \sigma}{2} + \left(\frac{1}{946.2} \cdot \frac{\Delta \sigma}{2} \right)^{\frac{1}{0.077}} , \tag{1}$$

$$\text{for } \underline{N_{s2}} : \frac{\Delta \epsilon}{2} = \frac{1}{221378} \cdot \frac{\Delta \sigma}{2} + \left(\frac{1}{887.2} \cdot \frac{\Delta \sigma}{2} \right)^{\frac{1}{0.082}}$$

and

Basic curves of low-cycle fatigue,

$$\frac{\Delta \epsilon}{2} = \frac{\sigma'_f}{E} N_f^b + \epsilon'_f N_f^c :$$

$$\text{for } \underline{N_{s1}} : \frac{\Delta \epsilon}{2} = 0.005105 \cdot N_f^{-0.061} + 0.0612 \cdot N_f^{-0.564} , \tag{2}$$

$$\text{for } \underline{N_{s2}} : \frac{\Delta \epsilon}{2} = 0.005117 \cdot N_f^{-0.065} + 0.0881 \cdot N_f^{-0.695}$$

Table 4 Coefficient of determination (R^2) in processing of the data from LCF tests of PM of NN-70

Specimen	$\Delta\varepsilon/2\%$	CSSC			BCLCF					
		n'	K'	R^2	b	σ_f'	R^2	c	ε_f'	R^2
		1 2	1 2	1 2	1 2	1 2	1 2	1 2	1 2	1 2
PM-01	0.35	0.047	946.2	0.66	-0.061	1130.1	0.77	-0.564	0.0612	0.72
PM-10	0.45	0.032	887.2	0.62	-0.065	1132.7	0.78	-0.695	0.0881	0.68
PM-03	0.50									
PM-06	0.60									
PM-07	0.60									
PM-05	0.70									
PM-08	0.80									

1 Method of the middle stabilization (ms), $N_{s1} = N_{bs} + (N_{es} - N_{bs})/2$

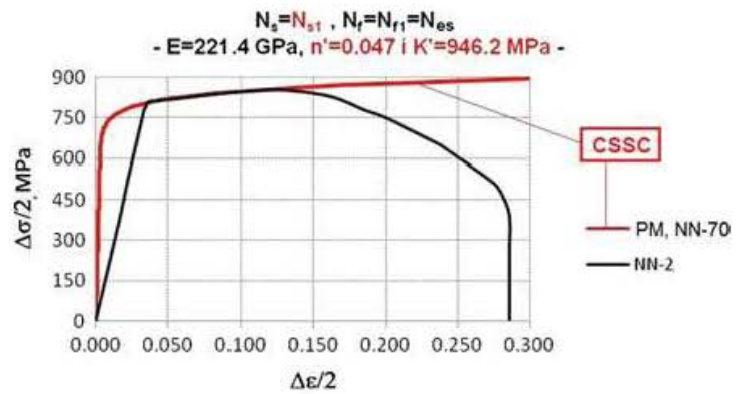
2 Threshold NDT method (tNDT), $N_{s2} = N_{bs} + (N_{tNDT} - N_{bs})/2$

Processing and Presentation of Test Results

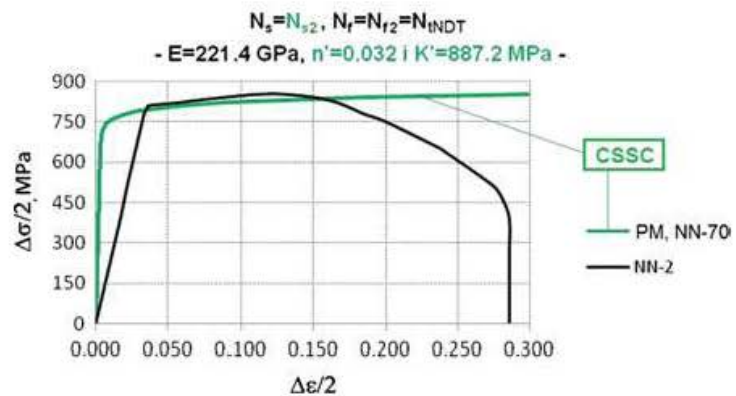
As a result of low-cycle fatigue test on one specimen (one amplitude level of strain) there is a record in the program EXCEL which, using the tools available in EXCEL, can be further processed according to our requirements [8]. Before processing of the results it is possible to roughly determine the cycle in which there is a significant drop of force, $N_{\text{estimated}}$. To determine the indicators of low-cycle fatigue of the material presented by cyclic stress-strain curve (CSSC) and basic curve of low-cycle fatigue (BCLCF), the following analyses of the results of low-cycle fatigue tests were made:

1. For each amplitude level of strain (each specimen), by filtering the data, extreme values of the load forces and number of cycles were paired, and thus we eliminated the excess data. Both positive and negative values of the load forces were filtered.
2. The diagrams of extreme values of the load forces and number of cycles (F-N curves) were drawn for each amplitude level of strain.
3. The diagrams of determination of the areas of stabilization, Fig. 4a, were drawn (positive part of the F-N curves, the area of stabilization, was determined by linearization of the data on maximum tensile forces of load in low-cycle fatigue tests for each amplitude level of strain, Table 3). The areas of low-cycle fatigue and characteristic hysteresis were defined after the following:
 - a. Determination of maximum force and starting cycle N_{start} ,
 - b. Determination of the cycle of start of stabilization, N_{ss} , end of stabilization, N_{es} , threshold of NDT, N_{tNDT} and area of stabilization,
5. The characteristic data of stabilized hysteresis curves, Fig. 4b, for each amplitude level of strain were defined:
 - a. Extreme values of load force F_{smax} and F_{smin} were read.
 - b. The spots of intersection of the hysteresis curve and positive part of strain axis were established in EXCEL (coefficients of the straight line, m and b [8] were determined). This can be done graphically [4], too, in some of the programmes for precision drawing. $\Delta \varepsilon_p/2$, $\Delta \varepsilon_e/2$, $A_0 = D^2 \cdot \pi/4$ (3), $F_{\text{mean}} = (| F_{\text{smax}} | + | F_{\text{smin}} |)/2$ (4) i $\Delta \sigma/2 = F_{\text{mean}}/A_0 \cdot 1000$ (5) values were calculated.
6. The data on all amplitude levels of strain were classified, cyclic stress-strain curves and basic curves of low-cycle fatigue were constructed [8, 15] and cyclic versus monotonous stress-strain curves compared, Figs. 5 and 6:
 - a. The exponents and coefficients were determined using linearized step function, n' and K' .
 - b. The exponents and coefficients were determined using linearized elastic component, b and σ'_f . The exponents and coefficients of linearized plastic component, c and ε'_f , were determined.

Fig. 5 Comparison of cyclic (CSSC) and monotonous stress-strain curve of PM of NN-70 steel



(a) $N_f = N_{f1}$ (End of stabilization [8])

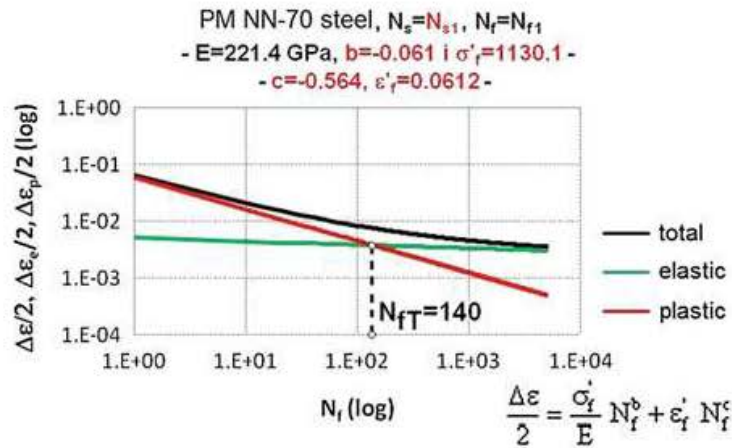


(b) $N_f = N_{f2}$ (threshold of NDT [8])

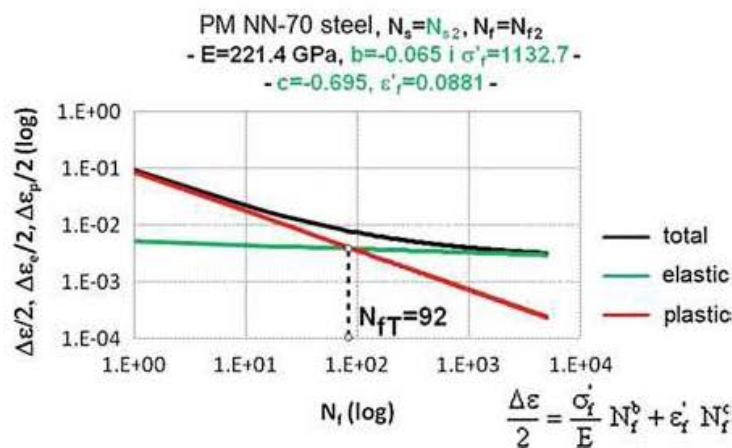
7. The data on cyclically stress-strain curves, Fig. 5a, b, and basic curves of low-cycle fatigue, Fig. 6a, b, were classified for the group of selected stabilized hysteresis, N_{s1} and N_{s2} , in order to construct them [8], and finally,
8. Transition life, N_{fT} , was determined for a group of selected stabilized hysteresis, N_{s1} and N_{s2} , Fig. 6a, b and Table 5 [8].

Conclusions

The theoretical, experimental and numerical research of the behaviour of low-alloy high-strength steels exposed to loading induced by low-cycle fatigue that are described in this paper are very complex research task. Extensive theoretical studies have required synthesis of knowledge in multiple engineering fields and disciplines, and numerical and experimental studies are an important part of this work. One of the goals of the research imposed itself during the processing of the results of experimental investigations, and is expressed through improvement of the methodology and methods of processing of the test results in order to establish a



(a) $N_f = N_{f1}$ (End of stabilization [8])



(b) $N_f = N_{f2}$ (threshold of NDT [8])

Fig. 6 Basic curve of low-cycle fatigue of PM of NN-70 steel

Table 5 Transition life of PM of steel NN-70

PM, NN-70	E, MPa	221378	Elastic part		Plastic part		N_{RT}
	N_f	N_p	b	σ'_f	c	ε'_f	
$N_{s1} = N_{ps} + (N_{ks} - N_{ps})/2$	$N_{ks} = N_{f1}$	N_{s1}	-0.061	1130.1	-0.564	0.0612	140
$N_{s2} = N_{ps} + (N_{pNDT} - N_{ps})/2$	$N_{pNDT} = N_{f2}$	N_{s2}	-0.065	1132.7	-0.695	0.0881	92
Transition life			$N_{RT} = \left(\frac{\varepsilon'_s}{\varepsilon'_f}\right)^{\frac{1}{c}} \quad (6)$				

N_{RT} is transition life of PM of steel NN-70, and we calculated it for two different methods

universal methodology for assessment of the behaviour of materials affected by low-cycle load. The results of experimental investigation have given us important information about the understanding of fatigue behaviour of HSLA steel, NN-70, and the newly applied methods and recommendations of standards as well have enabled the precise determination of characteristic stabilized hysteresis for each strain level. From certain characteristic stabilized hysteresis, based on defined

criteria, the data necessary for determination of the equations of characteristic curves of low-cycle fatigue have been collected, which show the difference between the values of exponents and coefficients defined by presented methodology depending on the method applied for the determination of stabilized hysteresis.

The results obtained represent practical contribution to estimation of the behaviour of low-alloy high-strength steel NN-70 exposed to the effects of low-cycle fatigue.

Acknowledgements This work is a contribution to the Ministry of Education and Science of the Republic of Serbia funded Project TR 35011.

References

1. Ferjaoui A, Yue T, Abdel Wahab M and Hojjati-Talemi R, 2015, *International Journal of Fatigue* 73, 66–76.
2. Kumar D, Biswas R, Poh LH and Abdel Wahab M, 2017, *Tribology International* 109, 124–132.
3. Bhatti NA and Abdel Wahab M, 2017, *Tribology International* 109, 552–562.
4. Resende Pereira KdF, Bordas S, Tomar S, Trobec R, Depolli M, Kosec G and Abdel Wahab M, 2016, *Materials* 9 639; <https://doi.org/10.3390/ma9080639>.
5. Hojjati Talemi R and Abdel Wahab M, 2013, *Tribology International* 60, 176–186.
6. ISO 12106:2003(E): Metallic materials-fatigue testing-axial-strain-controlled method, Geneva: ISO 2003, Switzerland.
7. ASTM E606-04, Standard practice for strain-controlled fatigue testing, ASTM International, West Conshohocken, Pennsylvania, USA.
8. Aleksić V., 2016, *Low-cycle fatigue of high-strength low-alloy steels*, The draft version of the doctoral dissertation reported on the Serbian, University of Belgrade, Faculty of Technology and Metallurgy, Belgrade.
9. Bulatović S., 2014, *Elastic-plastic behaviour of welded Joint of high-strength low-alloy in conditions of low-cycle fatigue*, Doctoral dissertation on the Serbian, University of Belgrade, Faculty of Mechanical Engineering, Belgrade.
10. Radović N., Drobnjak Đ., 2001, *Development of steels for fabrication on welded constructions with improved safety*, Welding and Welded Structures, vol. 46, No. 3, p. 81–92.
11. Grabulov V., 1986, A contribution to the assessment of chemical composition and plate thickness influence on crack initiation in welded joints made of Nionikral 70 steel, Master thesis on the Serbian, University of Belgrade, Faculty of Technology and Metallurgy, Belgrade.
12. Radović A., Marković D., 1984, *The conquest of shipbuilding steel of high-strength - NIONIKRAL-70*, The report in Serbian, Military Technical Institute, Belgrade.
13. Janković D. M., Malociklusni zamor, Univerzitet u Beogradu, Mašinski fakultet, Beograd, 2001.
14. Aleksić V., Aleksić B., Milović Lj.: *Methodology for determining the region of stabilization of low-cycle fatigue*, Book of Abstracts, 16th International Conference on New Trends in Fatigue and Fracture (NT2F16), May 24–27, 2016, Dubrovnik, Croatia, p. 189–190.
15. Aleksić V., Milović Lj., Aleksić B., Abubkr M. Hemer: *Indicators of HSLA steel behaviour under low-cycle fatigue loading*, 21st European Conference on Fracture, ECF21, 20–24 June 2016, Catania, Italy, *Procedia Structural Integrity* 2 (2016) 3313–3321.